



King Saud University
Arabian Journal of Chemistry

www.ksu.edu.sa
www.sciencedirect.com



ORIGINAL ARTICLE

Effect of amide-based compounds on the combustion characteristics of composite solid rocket propellants

Djalal Trache^{a,*}, Filippo Maggi^b, Ilaria Palmucci^b, Luigi T. DeLuca^b,
Kamel Khimeche^a, Marco Fassina^b, Stefano Dossi^b, Giovanni Colombo^b

^a UER Chimie appliquée, Ecole Militaire Polytechnique, BP 17, Bordj-el-Bahri, Algiers, Algeria

^b SPLab, Dept. of Aerospace Science and Technology, Politecnico di Milano, 34 Via La Masa, 20158 Milan, Italy

Received 13 September 2015; accepted 22 November 2015

KEYWORDS

Composite propellant;
Ammonium perchlorate;
Burning rate suppressant;
Combustion characteristics

Abstract Oxamide (OXA) and azodicarbonamide (ADA) are among the known burning rate suppressants used in composite solid rocket propellants. Much research has been carried out to understand mechanism of suppression but literature about the action of OXA and ADA on the combustion characteristics of propellant is still scarce. Here, a systematic study on coolant-based propellants has been undertaken spanning from thermal analyses of ingredients to a variety of burning processes of the corresponding propellants. Thermal gravimetric analysis and differential thermal analysis on individual coolants are carried out to study their behaviour with temperature. It was noticed that the thermal decomposition of OXA exhibits only endothermic effects, whereas that of ADA presents both endothermic and exothermic effects. Successive experiments on solid propellant looking at burning rate characterization, condensed combustion product collection and visualization, pressure deflagration limit and thermochemical analysis gave a greater insight and enabled better understanding of the action of coolants during combustion. It is proposed that OXA and ADA are acting on both the condensed and gas phases. Also, the nature of coolant is a key parameter, which affects the burning rate pressure index. Increase of agglomerate size and of pressure deflagration limit was obtained in the coolant-based propellants, confirming the trend given in the literature.

© 2015 The Authors. Production and hosting by Elsevier B.V. on behalf of King Saud University. This is an open access article under the CC BY-NC-ND license (<http://creativecommons.org/licenses/by-nc-nd/4.0/>).

* Corresponding author. Tel.: +213 661808275; fax: +213 21863204.

E-mail address: djalaltrache@gmail.com (D. Trache).

Peer review under responsibility of King Saud University.



Production and hosting by Elsevier

1. Introduction

Ammonium perchlorate-based composite solid propellants have been a workhorse in the field of solid rocket propulsion for more than six decades. This type of propellant presents not only excellent burning characteristics but also acceptable cost, processability and storability. Among other advantages and features, the ability to tailor ballistic properties can be achieved by modification of the propellant formulation and/or through use of various additives such as ballistic modifiers,

<http://dx.doi.org/10.1016/j.arabjc.2015.11.016>

1878-5352 © 2015 The Authors. Production and hosting by Elsevier B.V. on behalf of King Saud University.

This is an open access article under the CC BY-NC-ND license (<http://creativecommons.org/licenses/by-nc-nd/4.0/>).

Please cite this article in press as: Trache, D. et al., Effect of amide-based compounds on the combustion characteristics of composite solid rocket propellants. Arabian Journal of Chemistry (2015), <http://dx.doi.org/10.1016/j.arabjc.2015.11.016>

Nomenclature*Chemicals*

ADA	azodicarbonamide
ADN	ammonium dinitramide
Al	aluminium
Al ₂ O ₃	alumina
AP	ammonium perchlorate
GAP	glycidyl azide polymer
HTPB	hydroxyl terminated polybutadiene
OXA	oxamide

Acronyms

CCP	condensed combustion product
CEA	chemical equilibrium with application
cAP	coarse AP
CP	composite propellant
DTA	differential thermal analysis
fAP	fine AP
fps	frames per second
LEF	leading edge flame
MW	molar mass of combustion products

MF	molar fraction of condensed products
OB	oxygen balance
TGA	thermogravimetry analysis
TMD	theoretical maximum density

Symbols

D_{agg}	mean Al agglomerate diameter, μm
D_{43}	volume-averaged Al agglomerate diameter, μm
D_{32}	surface-averaged Al agglomerate diameter, μm
T_f	adiabatic flame temperature, K
ρ_p	propellant density, g cm^{-3}
I_s	specific impulse, s
ΔH_f	enthalpy of formation at standard condition, kJ/mol
n	burning-rate pressure exponent
P	pressure, bar
a	pre-exponent (multiplicative factor) of burning-rate law
r_b	propellant linear burning rate, mm s^{-1}

plasticizers, bonding agents, and stabilizers (Brewster and Mullen, 2010; Kohga and Okamoto, 2011; Kubota, 2007; Mezroua et al., 2014; Teipel, 2006).

Additives are usually added to the propellant formulation in small quantities. Their main function is to improve peculiar propellant features at the expense of some other parameters, looking for a compromise among properties. In general it is observed a decrease of the specific impulse (not more than 1%) due to their low energy content. Ballistic modifiers are additives that can be employed in few per cent ratios (between 0.5% and 3% of the oxidizer) in order to increase (as catalysts)/decrease (as coolants) the burning rate or reduce the sensitivity of the burning rate to temperature or pressure in a controlled manner (De la Fuente, 2013; Klager and Zimmerman, 1992). Composite solid propellants with high burning rate that produce a huge amount of combustion gases in a short period of time are often required to realize high performance rocket motors and would enable vehicles to fly at high speeds (for example: rockets and missiles). On the other hand, propellants with low burning rate engender low thrust, and are employed for instance as a slow burning rocket booster or a gas generator for controlling vehicle flight (Ghorpade et al., 2010; Ishitha and Ramakrishna, 2014; Parhi et al., 2015).

An ideal solid propellant should have stable burning rate and a low pressure exponent. To achieve this aim many efforts have been made, including the incorporation of coolants into propellant formulations. A wide variety of coolants, commonly called burning rate suppressants, have been tested such as ammonium chloride, ammonium polyphosphate, lithium fluoride, strontium carbonate, hexabromocyclododecane, diammonium bitetrazole and triphenyl antimony (Dey et al., 2014; Strunin et al., 2010). Other inorganic salts such as calcium carbonate, sodium carbonate and sodium bicarbonate have shown good burning rate retarding effects (Chai et al., 1995; Dey et al., 2014). Some explosives such as 3-nitro-1,2,4-triazol-5-one, 3-amino-5-1,2,4-triazole, nitroguanidine and triaminotrinitrobenzene have been reported as burning rate suppressants (Dey et al., 2014; Jawalkar et al., 2012; Williams et al., 1994). Further potential coolants including diaminoglyoxime, diaminofurazan, biuret, urea, melamine, oxamide and azodicarbonamide have also been investigated (Ghorpade et al., 2010; Salmon, 2006; Stoner and Brill, 1991; Talawar et al., 2005, 2006; Zhang et al., 2010). Amide-based compounds are most effective and are commonly

used as burning rate suppressants in practical applications of composite solid propellants. Yet the mechanisms of combustion in the presence of these additives are still poorly understood compared to the formulations containing diaminoglyoxime and diaminofurazan which have been widely investigated by several authors (Stoner and Brill, 1991; Talawar et al., 2005, 2006; Williams et al., 1994).

To the best of our knowledge, the investigation of the effect of amide compounds on the burning rate suppressant mechanism and the agglomerates size during combustion of aluminized solid propellants has not been described. Therefore, it seems appropriate to carry out a detailed study about the effect of these additives on the combustion characteristics of composite propellants. During this work, thermal studies on oxamide and azodicarbonamide were undertaken by applying simultaneous thermal analysis TGA-DTA. The combustion characteristics of AP/HTPB/Al composite propellants containing these additives were evaluated by theoretical calculation of performance and by determining strand-burning rate experimentally. The effect of these ballistic modifiers on the combustion agglomerates size and the pressure deflagration limit was also investigated.

2. Experimental*2.1. Propellant formulation*

Bimodal ammonium perchlorate (AP), coarse AP (cAP) and fine AP (fAP), was used as oxidizer in this study. The cAP had mean particles diameter of 200 μm and fAP was prepared by milling using a centrifuge grinder (Retsch S100) and featured a mean diameter of 10 μm , as determined by Malvern Mastersizer 2000 analyser. The metal powder, used as a fuel, was a commercial spherical μAl (with 30 μm nominal diameter). The binder was based on hydroxyl-terminated polybutadiene (HTPB R-45, Cray Valley), a polyfunctional oligomer of butadiene which comes with hydroxyl groups. The propellant was cured using an isocyanate and a tin-based catalyst. The baseline propellant formulated in the present investigation

AP/Al/HTPB contains 86 mass% total-solids with 58 wt.% cAP and 10 wt.% fAP. In the case of propellant formulations containing oxamide OXA (Sigma Aldrich) and azodicarbonamide ADA (Acros Organics), the coolant is used in place of cAP particles, so that the grand total of weight-based solid loading and the fAP/HTPB ratio are the same as in the corresponding baseline. This choice is driven by the consideration that fAP/binder ratio is a crucial factor that determines plateau burning rate trend and extinction characteristics (Jayaraman et al., 2009b). On the other hand, following the general expectation of decreased burning rates with the increased size of AP particles (Jayaraman et al., 2009a; Kubota, 2007), the burning rate suppressant effect of these additives could be confirmed. All the propellant formulations details are summarized in Table 1.

The propellant ingredients were weighted with <0.5% error. All propellant mixtures were produced in 100 g batches using a Resodyn LabRAM resonating mixer. Air bubbles trapped in the propellant slurry while mixing were removed by degassing in a vacuum-casting chamber. The mixed slurry was subsequently pressed into Teflon moulds, cured initially at 36 °C for 24 h, and followed by another curing at 60 °C for 48 h. Fig. 1 shows 5× optical microscopy images of the propellants surface. Visually, all the samples appear to be homogenous and well mixed. The images of the propellant surfaces show very clearly the well-dispersed AP crystals and no obvious distinction can be made in the images when the ballistic modifiers are added.

2.2. Measurement of thermal decomposition of coolants

The thermal decomposition of coolants used in the present work was carried out using a simultaneous TDA–TGA analyser (model SII Exstar 6000). The sample was placed in an alumina open crucible and instrument was calibrated against melting point and fusion enthalpies of indium, tin, lead, zinc and silver. The mass of each sample was in a range of 4–7 mg, which was heated from 50 to 500 °C under argon gas atmosphere with a heating rate of 10 °C/min. Data acquisition and processing were done with Muse version 2.0 software.

2.3. Theoretical performances determination

NASA's Computer Program for Calculation of Complex Chemical Equilibrium Composition and Application (CEA) (Gordon and McBride, 1996) was used to evaluate combustion chamber properties (namely, adiabatic flame temperature, specific molar fraction, molar mass, specific heat and so forth). The adiabatic flame temperature (T_f), the specific impulse (I_s),

the characteristic velocity (c^*), the molar mass of combustion products and the molar fraction of condensed products of the propellant were theoretically estimated under ideal conditions in the present survey.

In order to get a meaningful comparison between different performances data, a chamber pressure of 7 MPa, an ideal expansion to 0.1 MPa, and an initial temperature of 298 K were assumed. Physical and thermodynamic data of different ingredients used are listed in Table 2.

2.4. Measurement of propellant density

The densities of all propellant samples were measured using a Gibertini Europe 500 electric balance with a minimum reading of 0.001 g equipped with a kit for solid density measurement based on Archimedes principle. Ethanol 95% was used as the suspending medium. Each sample was approximately 10 mm in diameter and 10 mm in length. Three measurements were performed for each sample. The percentage gap (De Luca et al., 2014) between actual and maximum theoretical fuel density (due to porosity and other reasons) is defined by Eq. (1):

$$\Delta\rho_p = 100 \cdot \frac{\rho_{p,Actual} - \rho_{p,TMD}}{\rho_{p,TMD}} (\%) \quad (1)$$

2.5. Measurement of burning rate of propellants

The testing samples were cut out from propellant grains into rectangular strands measuring $30 \times 4 \times 4 \text{ mm}^3$, and side-inhibited to prevent lateral combustion. The burning behaviour was investigated in a pressurized nitrogen-flushed windowed bomb. Each strand was ignited using a hot nichrome wire. Pressure was kept constant during the whole combustion process with a feedback pressure control system. Steady burning rates were measured in the pressure range 0.5–4 MPa, using an automated image processing technique from a high-speed video recorder (Photron FASTCAM-APX 120KC). Videos were digitally post-processed using an in-house software for burning rate measurement (Hydra). At least three samples were used for each experimental point, according to well-established Space Propulsion Laboratory procedures (DeLuca et al., 2005). A typical example of propellant combustion is shown in Fig. 2, revealing that all of the tested formulations showed steady-state combustion and their burning surface was almost flat.

2.6. Measurement of agglomerates size

A high-speed and high magnification digital colour video camera, equipped with a long-range microscope, allowed slow motion observation of combustion phenomena with minimum interference with the combustion process. The propellant samples were about 15 mm tall and have cross-sectional dimension of $4 \times 2 \text{ mm}^2$ approximately. They are coated with a thin layer of low molecular-weight polymer to inhibit the sides from burning. Tests were carried out in a nitrogen-flushed chamber with optical view ports. Combustion occurred in a nitrogen atmosphere with the pressure regulated by an automatic control system. The images were captured at 1000 fps. Care was taken to exclude burning transients from video recording. Pixel-millimetre calibration was repeated for each test session.

Table 1 Mass fraction of the investigated propellant formulations.

Propellant	AP + Coolant	HTPB	Al	Coolant (% of cAP)	
				OXA	ADA
CP-Baseline	68	14	18	–	–
CP-OXA1	68	14	18	0.5	–
CP-OXA2	68	14	18	3	–
CP-ADA1	68	14	18	–	0.5
CP-ADA2	68	14	18	–	3

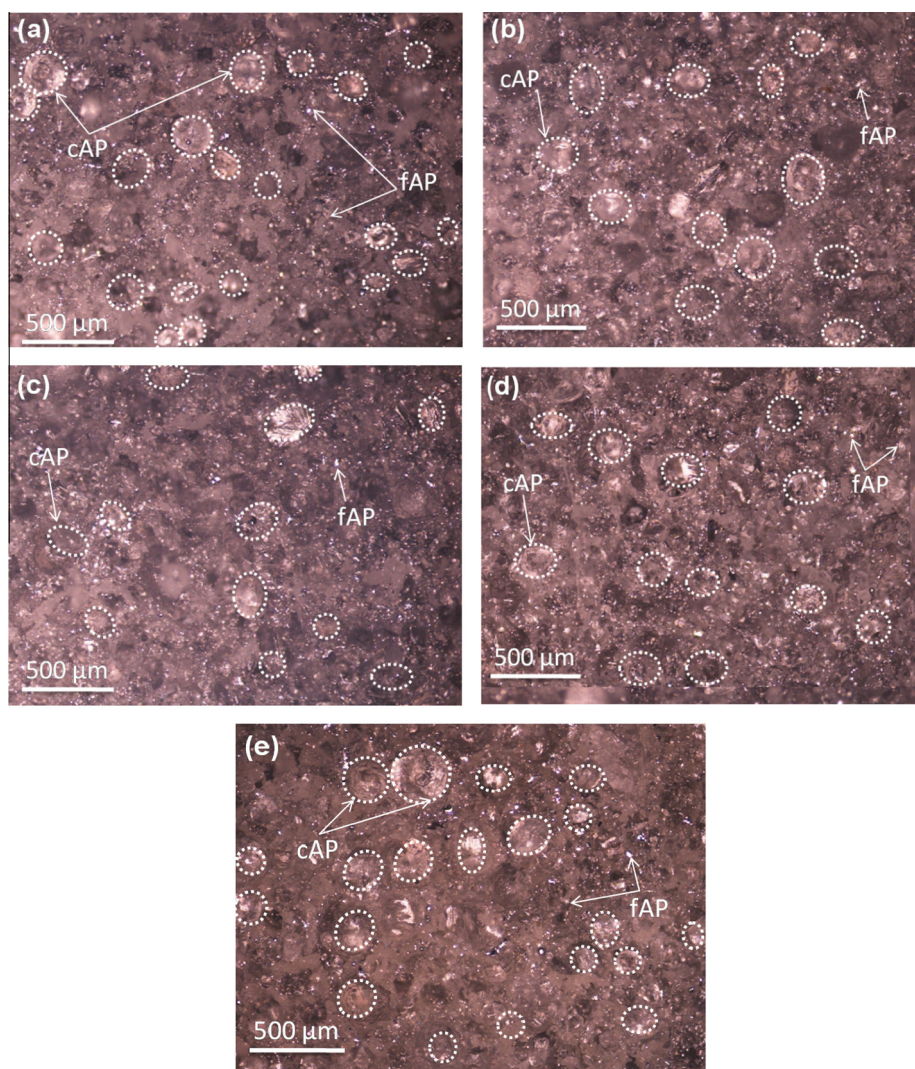


Figure 1 5×-Optical microscopy of: (a) CP-Baseline, (b) CP-OXA1, (c) CP-OXA2, (d) CP-ADA1 and (e) CP-ADA2 showing the well-dispersed AP crystals.

The agglomerate size on a burning surface was measured by analyzing the movie frames. The use of natural illumination for size determination must be treated with caution, as stated by Maggi et al. (2011) and Liu (2005). About 200 agglomerates were directly measured for each test. Similar approach was previously adopted by several authors (Grigor'ev et al., 1981; Liu, 2005). Arithmetic mean diameter D_{agg} and volume-weighted mean diameter D_{43} are computed.

$$D_{\text{agg}} = \frac{\sum n_i D_i}{\sum n_i} \quad (2)$$

$$D_{43} = \frac{\sum n_i D_i^4}{\sum n_i D_i^3} \quad (3)$$

2.7. Collection of combustion residues and particle size measurement

Several methods concerning the quenching and the collection of the combustion residues from the process of propellant sample burning have been proposed (Babuk et al., 1999; Glotov and Zyryanov, 1995; Jayaraman et al., 2011). The schematic

Table 2 Physical and thermodynamic data of propellant ingredients used for thermochemical analysis.

Ingredient	Formula	ρ (g cm ⁻³)	ΔH_f (kJ mol ⁻¹)	OB (%)	Reference
AP	NH ₄ ClO ₄	1.950	-296.00	+ 34.00	Kubota (2007)
HTPB	C _{7.073} H _{10.65} O _{0.223} N _{0.063}	0.920	-58.00	-315.17	Kubota (2007)
Aluminium	Al	2.700	0.00	-89.00	Teipel (2006)
OXA	C ₂ H ₄ N ₂ O ₂	1.667	-515.17	-72.67	Ghorpade et al. (2010)
ADA	C ₂ H ₄ N ₄ O ₂	1.650	-321.30	-55.17	Salmon (2006)

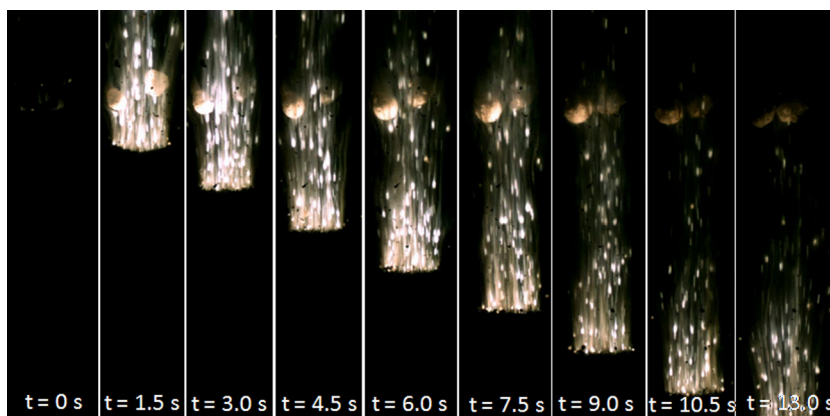


Figure 2 Selection of frames from combustion of CP-ADA1 at 1 MPa showing a steady-state combustion with a flat burning surface.

of the used quench collection set-up and the procedure, developed at Space Propulsion Laboratory, is given elsewhere (Galfetti et al., 2007; Meda et al., 2005). The particle size distribution of the dried quench-collected agglomerates was measured using Malvern Mastersizer 2000 analyser equipped with a dry powder dispersion unit (Scirocco) from 0.1 to 2000 μm .

2.8. Measurement of pressure deflagration limit

Pressure deflagration limit (PDL) has been conventionally determined as the pressure below which a flame does not propagate without adding energy to the system. The practical aim to study the PDL phenomenon is associated with the likelihood of controlling the important process of ignition and extinction. This is a crucial parameter since the safe storage handling and transportation of solid propellants required more complete information on the effect of the nature of propellant and the operating conditions, in order to avoid accidents and ensure permanent extinction of the propellant during these circumstances. Moreover, the steady-state combustion of propellant systems with ballistic modifiers at subatmospheric pressures supports the understanding of combustion-wave propagation under conditions, having a minor contribution from gas-phase reaction.

The details of the technique used to measure solid propellant PDL are given elsewhere (DeLuca et al., 1992; Zanotti and Giuliani, 1994).

3. Results and discussion

3.1. Thermal behaviour of ballistic modifiers

To understand the effect of amide-based components on the combustion characteristics of composite solid propellants we first looked at the decomposition of single coolants. Fig. 3(a) exhibits the TGA–DTG curves of ADA and OXA used in this work. The ADA showed three thermal decomposition stages in the temperature ranges of 200–240 °C, 242–260 °C and 265–355 °C, whereas the OXA showed two clearly separated steps in the temperature ranges of 150–200 °C and 220–275 °C. Maximum weight losses, corresponding to the first decomposition stage of ADA and to the second decomposition step of OXA, were of the order of 55% and 91%, respectively. The obtained results indicated that a complete decomposition of

the two compounds took place without final residues. All the data are listed in Table 3.

The output of DTA for ADA and OXA is depicted in Fig. 3 (b). ADA features two exothermic peaks in the ranges of 200–235 °C and 305–345 °C and one endothermic peak in the temperature range of 240–260 °C, which indicated that the complete thermal decomposition of ADA occurred in different steps. These results are in good agreement with the literature data (Reyes-Labarta and Marcilla, 2008; Robledo-Ortiz et al., 2008; Zhang et al., 2010), where the formation of low molecular weight gases H_2 , CO, N_2 and cyanic acid was confirmed according to three competitive reactions. On the other hand, two decomposition processes, both endothermic, occur between 150 °C and 300 °C, showing a maximal rate at 274 °C for OXA. According to the literature (Langbein and Mayer-Uhma, 2009; Tayler and Bircumshaw, 1956), OXA is decomposed to NH_3 , CO and HCN gases. Consequently, the NH_3 thermal decomposition produces H_2 and N_2 (Dirtu et al., 2006).

3.2. Solid propellant performance analyses

The theoretical performance parameters I_s , T_f , c^* and combustion products composition from NASA CEA code for the investigated propellants are given in Tables 4 and 5. In general, performance parameters decreased with the increase of the coolant (AZO or OXA) content since ingredients with negative oxygen balance are introduced in the formulation. No significant effect appeared when 0.5 wt.% coolant was added. As shown in Table 4, the computed T_f of CP-Baseline is 3404 K at 7 MPa, but is reduced to 3326 K or 3344 K due to the partial replacement of ammonium perchlorate with either 3 wt.% OXA or 3 wt.% AZO, respectively. This lower adiabatic flame temperature decreases the ideal specific impulse from 315.2 s (without coolant) to either 312.5 s (3 wt.% OXA) or 313.3 s (3 wt.% AZO). This fact suggests that the burning rate might be decreased by a reduction of the flame temperature and, thus, of the heat feedback, unless exothermic superficial reactions occur.

Table 5 lists the theoretically estimated main combustion products from the propellants. No significant influence was found once 0.5 wt.% of coolants was used. For the propellants containing 3 wt.% of coolants, the mole fraction of H_2 , CO and N_2 is notably increased, indicating that the amide-based components contained in the propellant can burn. This result agreed with the abovementioned thermal decomposition of

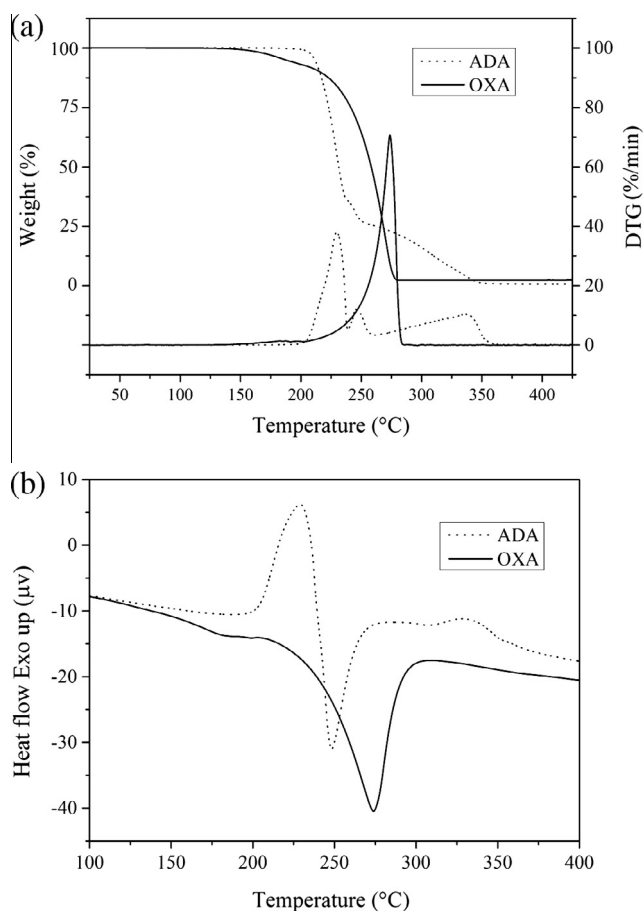


Figure 3 (a) TGA/DTGA and (b) DTA curves of coolants with a heating rate of 10 °C/min showing their thermal behaviour.

Table 3 Simultaneous TGA/DTA data obtained for the investigated ballistic modifiers.

Sample	Stage	TGA			DTA	
		Onset (°C) ^a	Peak (°C) ^b	Wt (%) ^c	T_i (°C) ^d	T_m (°C) ^e
ADA	1	206.0	237.8	55.07	204.2	229.1
	2	240.2	245.0	13.83	243.7	248.3
	3	299.6	340.4	31.10	315.8	328.2
OXA	1	167.6	187.7	8.49	163.3	203.1
	2	237.4	271.6	91.51	243.5	274.0

^a Onset decomposition temperature using TGA results.

^b Peak temperature of DTG.

^c Residual weight.

^d Onset decomposition temperature using DTA results.

^e Peak temperature using DTA results.

coolants. The fractions of H₂O and HCl are smaller than those for the CP-Baseline. Chlorine is delivered by ammonium perchlorate so its partial replacement causes a decrement of Cl atom availability. Consequently, the exhaust combustion product contains less smoke-producing constituents. The Al₂O₃ mole fraction is almost constant in all of the investigated formulations.

3.3. Propellants characterization

3.3.1. Propellants density

The measured density values of the produced propellants are listed in Table 6. No apparent deviation of the propellant densities with the coolants content was found since the density of latter was very close to that of the composite materials. The experimental density of propellants almost agreed with their theoretical values.

It is well known that the presence of bubbles causes the increase of the burning rate (Shioya et al., 2014). However, the open porosity of the prepared samples does not exceed 2%; hence, it is negligible, which indicates that the samples homogenization has been successfully completed and suggests the good ability of the binder to wet the entire surface area of the solid ingredients during propellant mixing.

3.3.2. Combustion properties of composite propellants

The pressure dependence of the burning rate r_b was evaluated, in accordance with the so-called Vieille's law, as $r_b = a \cdot P^n$, where n is the pressure exponent and a the multiplicative factor dependent on the propellant chemical composition and the initial propellant temperature (Chaturvedi and Dave, 2015). The obtained results are summarized in Table 7. The burning rates increased almost linearly with pressure on the logarithm scale, in the investigated pressure range.

3.3.2.1. Effect of ADA on the burning rate. Fig. 4(a) shows the burning rates obtained for the ADA-based propellants at various pressures. It can be observed that the CP-Baseline and CP-ADA2 propellants burning rate pressure dependencies (0.459 and 0.470, respectively) are nearly identical; however, their pre-exponents (1.110 and 0.935) differ appreciably. At atmospheric pressure, a significant decrease of burning rate is observed. This reduction, compared to the baseline formulation, corresponds to 16% for CP-ADA2 (Table 7). However, this decrease became smaller and corresponds to 12% at 7 MPa. Similar trend was given in the literature. Kubota (2007) reported that the use of 2% lithium fluoride in composite propellant grains leads to a decrease of 14% in the burning rate at 7 MPa. Kubota (2007) demonstrated that the use of 2% strontium carbonate to composite propellant decreased the burning rate at about 41% at 7 MPa. Ghorpade et al. (2010) showed that the incorporation of 10% of picrite, melamine or urea in composite solid propellant formulations diminished the burning rate of 18%, 50% and 46%, respectively at 7 MPa. In another work performed by Dey et al. (2014), they found that the addition of 10% of biuret to composite propellants caused a decrease of 33% in the burning rate at 7 MPa.

Composite solid propellant burns with both premixed and diffusion flame and the dominance of each of these flames determines the burning rate pressure exponent of the propellant (Beckstead et al., 1970; Ishitha and Ramakrishna, 2014). In conventional AP-HTPB propellants, the burning rates are controlled by the hot near-surface leading edge of the final diffusion flame (LEF) in which the oxidizer/fuel vapours react. These LEFs are anchored over the contact surface between sufficiently coarse AP particles and the surrounding binder, at any given pressure (Jayaraman et al., 2009b). As the ADA particles are included at the expense of the large AP particles, the LEFs over the burning surface become less prevalent,

Table 4 CEA calculated values of I_s , T_f , c^* , MW and MF.

Propellant	I_s (s)	T_f (K)	c^* (m s ⁻¹)	MW (g mol ⁻¹)		MF (%)	
				Chamber	Exit	Chamber	Exit
CP-Baseline	315.2	3404	1583.6	25.8	26.3	7.76	8.76
CP-OXA1	314.7	3390	1582.1	25.7	26.2	7.76	8.73
CP-OXA2	312.5	3326	1574.0	25.4	25.8	7.72	8.61
CP-ADA1	314.9	3393	1582.6	25.7	26.2	7.75	8.74
CP-ADA2	313.3	3344	1577.5	25.5	25.9	7.70	8.64

Table 5 Computed mole fractions of combustion products of investigated propellants.

Propellant	Mole fraction (%)							
	CO	CO ₂	H ₂	H ₂ O	N ₂	HCl	Al ₂ O ₃ ^a	Other
CP-Baseline	24.5	0.90	31.8	9.4	7.6	12.9	7.8	5.9
CP-OXA1	24.7	0.89	31.4	9.1	7.6	12.7	7.8	5.8
CP-OXA2	25.6	0.76	32.9	7.8	7.8	12.4	7.7	5.0
CP-ADA1	24.7	0.87	31.3	9.2	7.7	12.7	7.8	5.8
CP-ADA2	25.3	0.76	32.6	7.9	8.2	12.3	7.7	5.2

^a Solid state.**Table 6** Densities of the manufactured propellant samples.

Propellant	ρ_p (g cm ⁻³)	TMD (g cm ⁻³)	ρ_p /TMD (%)	$\Delta\rho_p$ (%)
CP-Baseline	1.727	1.761	98.1	1.9
CP-OXA1	1.738	1.761	98.7	1.3
CP-OXA2	1.740	1.762	98.8	1.2
CP-ADA1	1.736	1.760	98.6	1.4
CP-ADA2	1.733	1.755	98.7	1.3

contributing to a decrease in the burning rate. Different researchers have examined different aspects of combustion or of the flame structure. Fig. 5 is a schematic of the solid propellant flame structure that has been proposed in the present study. The concepts that are illustrated in Fig. 5(a) and (b) are specific to an ADA-based composite propellant. The figures illustrated the reaction zones that must be considered in order to understand the complex combination of mechanisms that occur in propellant combustion. The different phenomena explained in these schemes corroborate with the burning rate results and they are in accordance with the agglomerates size determined by an optical technique (where the combustion

of Al particles is observed on the surface), the agglomerates size determined by a quenching method (where the combustion of Al particles is observed in the gas phase) and the thermal analysis results as they will be discussed later in the paper.

The thermal decomposition of ADA starts with an exothermic reaction at around 204.2 °C (Fig. 3(b)) which could promote the decomposition of AP particles and might enhance the regression rates of AP by reducing its decomposition temperature. Aspects related to thermal behaviour of the studied propellants, such as thermal degradation, will be addressed in detail in a separate paper. Two exothermic decompositions are present, as observed in TGAs. The first decomposition is 352.6, 344.7 and 333.9 °C for CP-Baseline, CP-ADA1 and CP-ADA2, respectively. These results imply that ADA acts on AP condensed phase. Besides, the HTPB-IPDI based binder, which decomposes slowly between 300 and 360 °C (Chakravarthy et al., 1997), generates a thin melt layer; thus, the relative burning surface area of AP particles at the solid-gas interface is important and also, the fuel vapours have to travel just a short distance in order to get oxidized. This will lead to a higher n . This increased pressure exponent dependence (from 0.459 for CP-Baseline to 0.490 for CP-ADA1) is believed to be a result of the greater influence of kinetics that likely occurs between the oxidant species and the fuel vapours burning relatively close to the surface. We can deduce from the above discussion that ADA plays initially a catalytic effect. On the other hand, a further increase on the temperature of the surface leads to the second decomposition of propellant. The TGA results corresponding to this decomposition give 441.6, 448.0 and 451.1 °C for CP-Baseline, CP-ADA1 and CP-ADA2, respectively. It can be noticed that the complete decomposition of ADA, generating an important volume of inert diluents such as N₂, could possibly change the composition of reactants reaching the gas-phase and causes the decrease of the flame temperature. These gases can significantly inhibit the heat flow from the gaseous combustion zone back to the condensed phase and thus slow down the thermal decomposition, deflagration of AP and the fuel vapours have

Table 7 Comparison of burning rates (r_b) for the tested propellant formulations.

Propellant	a	n	R^{2a}	r_b (mm s ⁻¹)		
				0.5 MPa	4 MPa	7 MPa
CP-Baseline	1.110 ± 0.068	0.459 ± 0.030	0.979	2.32	6.03	7.80
CP-OXA1	1.217 ± 0.043	0.414 ± 0.010	0.998	2.36	5.60	7.07
CP-OXA2	1.234 ± 0.126	0.384 ± 0.029	0.985	2.28	5.08	6.31
CP-ADA1	0.986 ± 0.023	0.491 ± 0.015	0.995	2.17	6.03	7.91
CP-ADA2	0.935 ± 0.047	0.470 ± 0.017	0.993	1.99	5.29	6.89

^a Linear regression coefficient.

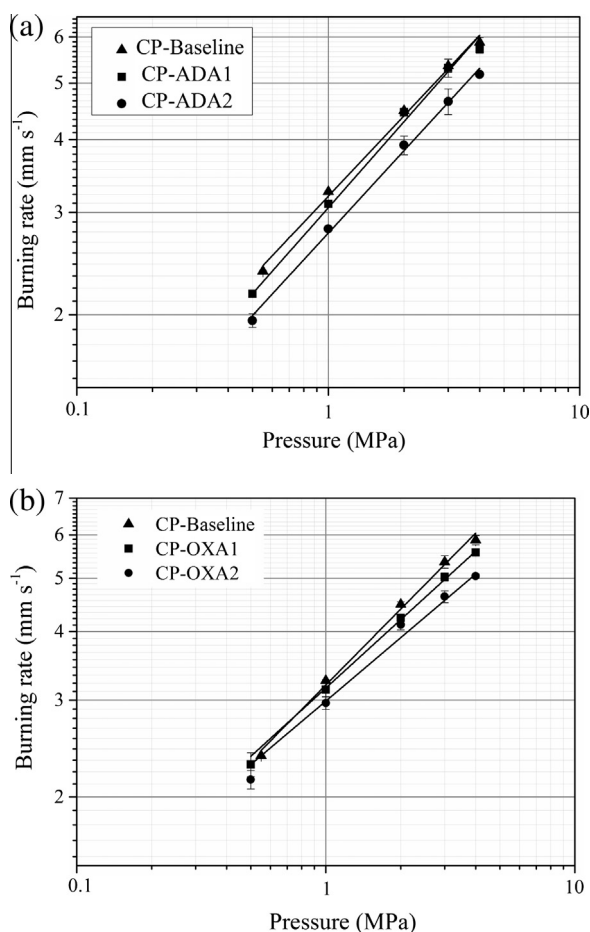


Figure 4 Solid propellant linear burning rates measured in a constant pressure strand burner: (a) ADA-based propellants, (b) OXA-based propellants showing faster combustion for the CP-Baseline.

to travel a large distance in order to get oxidized and diffusion becomes dominant. This has been argued to be due to the volume of inert gases released by ADA. More inert gases were released by CP-ADA2 ($n = 0.470$) compared to CP-ADA1 ($n = 0.490$). Consistent with findings presented here, it has been shown elsewhere that diffusion-controlled burning results in lower burning rate pressure dependence compared to kinetically controlled burning.

3.3.2.2. Effect of OXA on the burning rate. All the prepared formulations burn over the entire pressure range tested. Fig. 4(b) displays the burning rates obtained for the OXA-based propellants. It can be observed that the CP-Baseline and CP-OXA2 propellants pre-exponents (1.110 and 1.234) are almost identical; however, their burning rate pressure dependencies (0.459 and 0.384, respectively) change considerably. As discussed in the previous section for ADA, lower burning rate is observed for propellants once coarse AP is replaced by OXA. A decrease of 19% in the burning rate was found when 3% OXA is added at the expense of cAP at 7 MPa. This result corroborates with those obtained by common effective coolants where the burning rate reduction of composite propellants varied between 14% and 50% (Dey et al., 2014; Ghorpade et al., 2010; Kubota, 2007). The processes contributing to decrease the

burning rate of OXA-based propellants are similar to those schematically depicted in Fig. 5(b).

It should be recorded here that the addition of OXA to the propellant samples inhibits the decomposition processes. The thermal decomposition of OXA is an endothermic phenomenon, where the first endotherm starts at 163.3 °C and the main decomposition product is NH_3 , as already mentioned above. The abundance of NH_3 (g) causes suppression of the oxidizer sublimation, leading to deceleration of both condensed-gas-phases reactions occurred in the propellant surface. These conclusions confirm the obtained TGAs, where two exothermic decompositions were visible for OXA-propellants. The first decomposition is 352.6, 359.1 and 361.2 °C for CP-Baseline, CP-OXA1 and CP-OXA2, respectively. Thus, as the OXA content increases the decomposition of propellant decreases. The second decomposition of OXA propellants follows the same trend as the first one. The TGA results corresponding to this decomposition give 441.6, 449.2 and 452.0 °C for CP-Baseline, CP-OXA1 and CP-OXA2, respectively. These findings can be explained by the inhibition action of the decomposition process in the condensed-phase and the important volume of inert diluents such as N_2 reaching the gas-phase. Therefore, the flame temperature will be decreased and subsequently affects the heat feedback to the propellant surface. Diffusion controlled combustion dominates and this justifies the lower pressure exponent of OXA-based propellants.

3.3.3. Agglomerate sizes of propellant formulations

In a typical composite solid propellant, the aluminium particles are small compared to the cAP and hence are concentrated in pockets between oxidizer particles. During the combustion process, the aluminium particles are able to be warmed up before reaching the burning surface. These particles are only partially melted and are dispersed in a pyrolyzing fuel environment, where they are temporarily stuck in the binder melt. They are not instantaneously ignited because they are protected by a refractory Al_2O_3 coating and because of their fuel-rich environment. At the pocket sites Al particles continue to emerge and collect on the receding surface until they inflame and/or detach from the surface as agglomerates (DeLuca et al., 2010; Price, 1984).

The whole sequence is clearly illustrated in Fig. 6, showing the transition process for CP-ADA1 at 1 MPa. It can be seen that micron-sized aluminium used for the present set of experiments, gives larger agglomerate with respect to nano-sized aluminium as it is generally agreed in published works (DeLuca et al., 2010; Galfetti et al., 2007). The observed average agglomerate size for each propellant is summarized in Table 8. An increase of agglomerate size by 37% and 32% for CP-OXA2 and CP-ADA2, respectively, at 1 MPa respect with CP-Baseline is obtained. This increase is reasonable for composite propellant, since similar trend was previously reported by DeLuca et al. (2010) for other propellant formulations. The pressure effect is monotonic, finding larger agglomerates at low pressure.

It is shown in the previous section that the incorporation of OXA leads to thick melt-layer at the burning surface of propellant, compared to that obtained for ADA-propellants. Consequently, Al particles will form molten pools as they reach the burning surface, which agglomerate into larger droplets, or, alternatively, form large droplets through sinter and/

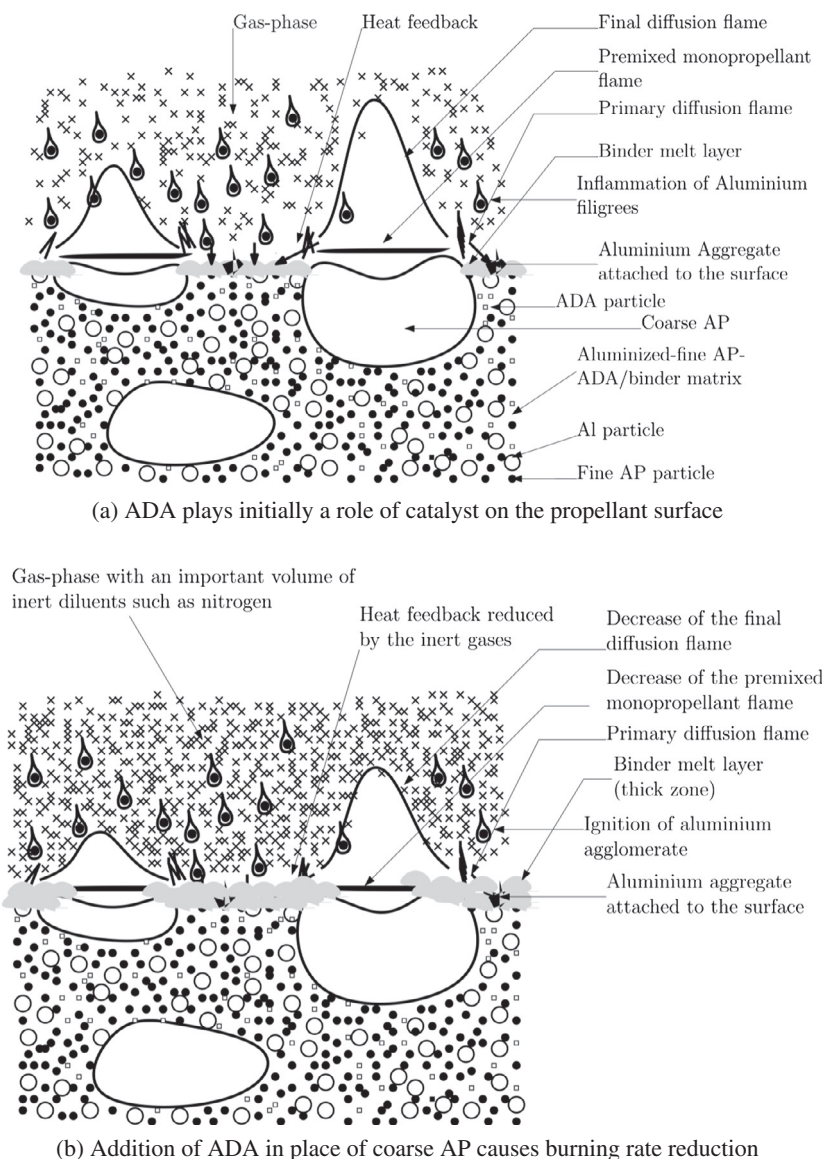


Figure 5 Processes' contribution to decrease the burning rate of ADA-based propellants.

or coalescence mechanism. Liu (2005) reported similar effect of melt-layer for propellant containing RDX on the agglomerate size data.

On the other hand, it is pointed out that the agglomeration size varies inversely with the propellants burning rate. Consequently, the agglomerate size increases correspondingly near the burning surface with the coolant content. Moreover, it is reported in the literature that the LEFs are the principal source of ignition of the aluminium particles that accumulate on the burning surface (Jayaraman et al., 2009b). Thus, it seems reasonable to consider that the decreased feedback caused by OXA decomposition either in condensed-phase or in gas-phase increases the tendency for surface retention-accumulation of aggregates. Subsequently, the agglomerates carried away with the outward vapour flow, will be characterized by large size than those of CP-Baseline. Furthermore, the accumulating aluminium particles (filigrees or clusters) act as thermal sink of the heat feedback from the gas-phase flame to the

propellant surface, contributing to a further decrease in the burning rate. These processes should prevail when more OXAs are added as well. Similar trend is obtained when ADA is used as coolant in the propellant formulations, but less appreciable change is observed in the size of the agglomerates, which indicates that a slight catalytic effect of ADA reduces the surface residence times of the droplets. However, the agglomerate size of the CP-Baseline is lower than that of the coolant-based propellants due to the decrease of the combustion rate of the droplets near the burning surface saturated with inert gases released by the coolants. A monotonic trend of agglomerate size decrease and the increase of pressure is also observed in this case. This latter observation is in agreement with that reported by Babuk et al. (1999).

3.3.4. Condensed combustion products (CCPs) analysis

First it is necessary to clarify that residuals observed by strand burner using optical technique (previous section) present

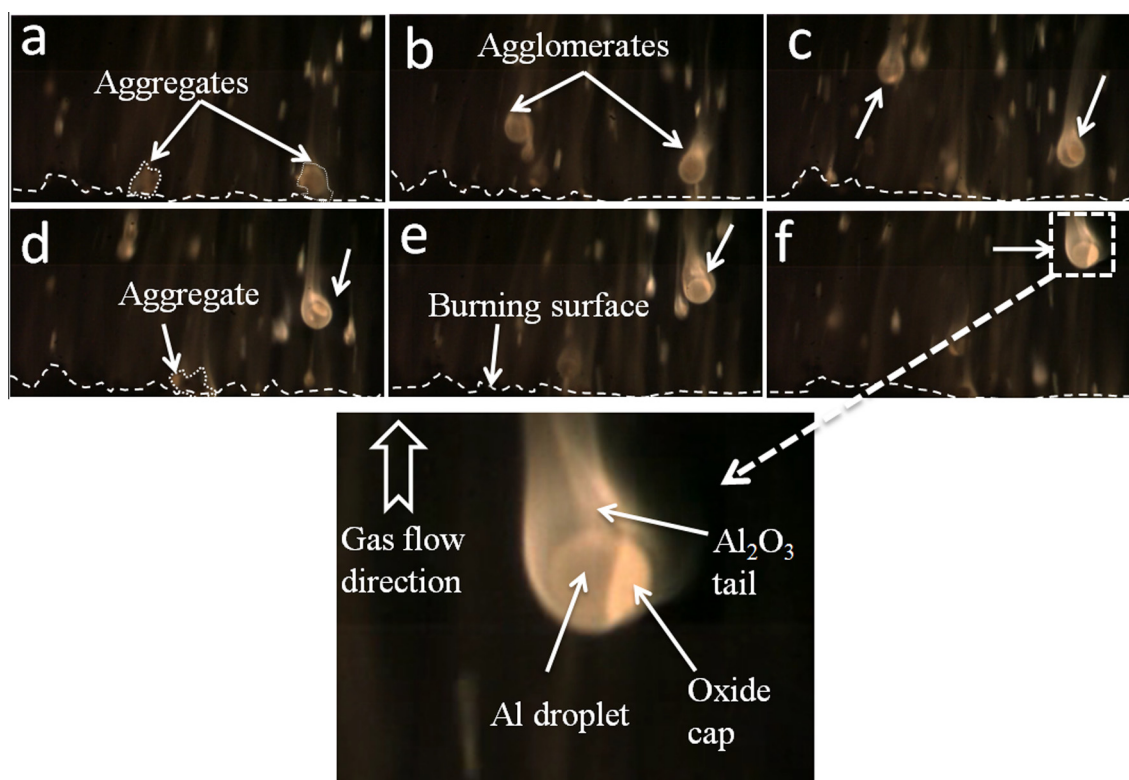


Figure 6 Image sequence capturing aggregate to agglomerate conversion for CP-ADA at 1 MPa.

Table 8 Agglomerate average diameters measured for the tested formulations.

Propellant	1 MPa		2 MPa	
	D_{agg} (μm)	D_{43} (μm)	D_{agg} (μm)	D_{43} (μm)
CP-Baseline	91.2 ± 4.1	112.0	74.4 ± 2.7	85.4
CP-OXA1	116.6 ± 4.4	139.4	103.1 ± 4.2	132.8
CP-OXA2	141.6 ± 4.0	153.0	116.4 ± 4.4	134.1
CP-ADA1	106.0 ± 5.3	134.8	98.5 ± 5.3	129.1
CP-ADA2	121.3 ± 5.6	148.5	106.2 ± 5.0	130.5

different features with respect to the ones obtained by a strand burner using a quenching technique. The reason for a lower particle size in this later method is that the optical technique has a lower threshold for the analysis of agglomerates and focuses on larger droplets while the collection technique includes in the measurement also particles having submicrometric size. Subsequently, the mean diameter size of agglomerate obtained with this technique is often lower. D_{43} at 1 MPa obtained with the optical technique for all of the investigated propellants is higher than that obtained with the quenching method (Tables 7 and 8). Depending on the working conditions and propellant formulation, CCPs ejected from the burning surface may have initial sizes in the range 10 to 200–800 μm with one to three-modal distributions covering a wide grain size distribution range (De Luca et al., 2014). The chemical composition of CCPs was not treated here, but important details were recently reported (De Luca et al., 2014).

Combustion of metalized solid propellants results in the formation of CCPs, which have an essential influence on

rocket motor performance. CCPs can be classified into two basic fractions: agglomerates and smoke oxide particles (Babuk et al., 1999). Representative size distributions of the collected CCPs residues, in agreement with the previous results (Cerri et al., 2007), are shown in Fig. 7(a) and (b) for two different values of the combustion pressure. The CCPs size distribution could be considered bi-modal. Data obtained in these figures show that part of condensed products presents a very fine grain size distribution around 1 μm . Similar conclusion was previously reported for aluminized solid propellant (De Luca et al., 2014).

The experimental data are summarized in Table 9. (1) For low coolant content (0.5%), it is well known that the skeleton layer plays a key role in the agglomeration process of metalized propellants. Moreover, theories (Babuk et al., 2005, 1999; Cohen, 1983; Sippel et al., 2014) suggest that agglomeration process could be affected by several parameters such as the nature of mechanism (pocket, prior-to-pocket and inter-pocket), the presence of a heterogeneous burning mode (on the surface) and a homogeneous burning mode (on the gas phase), and the non-stationary effects consisting of destruction of the particles by their gasification products because of the high rate of evaporation. Once a low quantity of coolant is added to the propellant formulations (CP-ADA1 and CP-OXA1), a minor effect is caused by the nature of agglomeration mechanism, whereas, the effect of last two factors is prevalent, contributing to agglomerate size (D_{43}) decrease (for instance, CP-OXA compared to CP-Baseline at 1 MPa) or increase (for instance, CP-OXA1 compared to CP-Baseline at 3 MPa). This competition between burning modes, as well as non-stationary effects is mainly governed by the volume of inert gases released by the coolant decomposition and

the flame temperature. The actual meaning of these data is however subject to uncertainty. (2) For high content of coolant (3%), the volume of inert diluents released during ignition becomes important and decreases the availability of oxidizer species for the Al by reducing the diffusion *i.e.*, enhancing the diffusional distances between the oxidizer and Al fuel. Oxidation of Al requires both the ignition of particles and the presence of oxidizing species. Both of the aspects are correlated to local temperature and composition. Consequently, agglomerate size is increased as reported in Table 8 for CP-ADA2 and CP-OXA2 compared to CP-Baseline.

3.3.5. PDL analysis of propellants

Steady-state deflagration occurs when the heat flux from all chemical reactions, including the gas-phase flame and the surface reactions back into the solid, is equal to the heat flux necessary to heat the solid from the ambient temperature far from the burning surface.

Experimental results indicate that the shape factor, defined as the area/perimeter ratio of the strand cross section, has an important effect of the PDL (Bruno et al., 1985; Sutton and Biblarz, 2010). The lowest PDL is reached when strands of larger cross section are used. The general and widely verified trend of PDL decrease with shape factor increase, shown in

Fig. 8, and the approach of the PDL to an asymptote confirms the dependence of PDL on the operating conditions and propellant composition.

As shown in Fig. 8, the propellants based on coolants have higher PDL values compared to the CP-Baseline at all shape factors. PDL increases with the increase of the coolant content in the propellant formulations. This result is attributed to both the effects of the reduced feedback and the decreased burning rate. This conclusion agreed with results reported by Peterson et al. (1967) who observed that increasing the binder level increased the PDL value and the high binder level reduced the AP that can deflagrate as monopropellant. Other investigators reported also that additives and ballistic modifiers affect the PDL (Krishnan and Swami, 1998). Furthermore, it is noticed that the use of OXA than ADA as coolant gives a higher PDL that is attributed to the important melt-layer on the propellant surface during combustion. Steinz et al. (1969) indicated that the relative meltability of the fuel is the major determining factor of the PDL and it increases with increasing ease of fuel melting. These conclusions corroborate with the results reported in the previous sections.

Under subatmospheric conditions, the investigated coolant-based propellants demonstrated a stable burning with a slight increase of PDL values. This indicates that these propellants are suitable for subatmospheric applications as well.

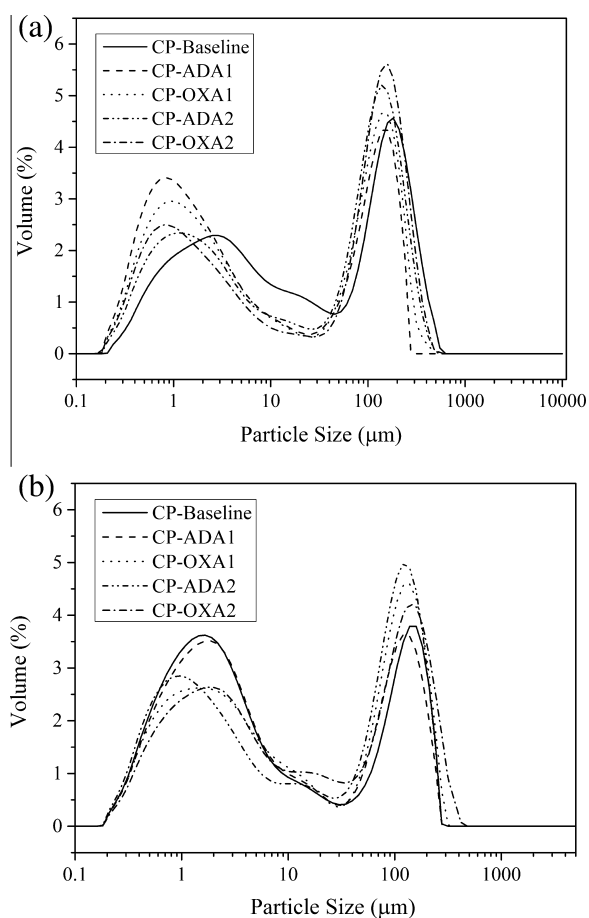


Figure 7 Qualitative character of the size distributions of condensed combustion products of aluminized propellants (with or without coolants): (a) at 1 MPa, (b) at 3 MPa.

Table 9 CCPs average diameters measured for the tested formulations.

Propellant	1 MPa		3 MPa	
	D_{32} (μm)	D_{43} (μm)	D_{32} (μm)	D_{43} (μm)
CP-Baseline	2.64	80.44	1.74	46.14
CP-OXA1	1.79	67.27	2.03	58.65
CP-OXA2	2.05	91.25	2.25	66.58
CP-ADA1	1.51	52.86	1.82	44.13
CP-ADA2	2.29	82.85	1.85	58.53

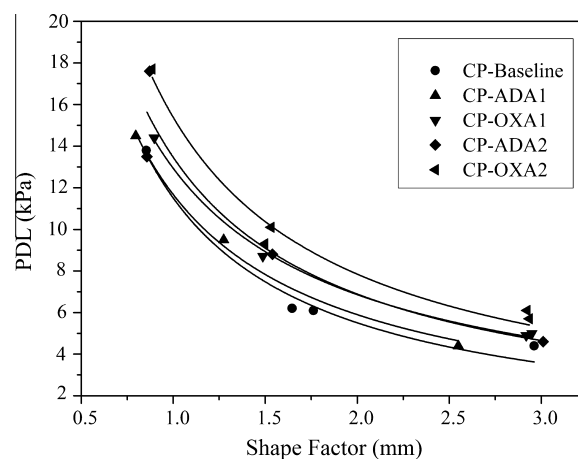


Figure 8 PDL versus shape factor for the investigated propellants showing higher PDL values for coolants-based samples compared to the CP-Baseline at all shape factors.

4. Conclusions

AP/HTPB-based aluminized solid rocket propellants, containing amide-based components as coolants, show slower steady burning rates compared to the corresponding composition containing only AP/HTPB/Al. This behaviour is in accordance with that reported for other burning rate suppressants (Dey et al., 2014; Ghorpade et al., 2010; Kubota, 2007). The oxamide-based aluminized propellants offer lower burn rate and pressure exponent values as compared with the propellants containing azodicarbonamide. The simultaneous thermal analysis of individual coolants indicated the different decomposition phenomena, involving only endothermic processes for OXA and endothermic/exothermic processes for ADA. It is pointed out that this different behaviour plays a key role on the action of these ballistic modifiers on the condensed-gas-phases. The incorporation of ADA causes firstly a catalytic effect of the propellant decomposition on the surface followed by an inverse action, whereas OXA reduces the propellant decomposition during overall processes. Additionally, the presence of coolants can produce agglomerates slightly larger than those of CP-Baseline. Finally, the propellant formulations containing these ballistic modifiers could be used under subatmospheric operations as well.

Future efforts should be focused on use of suitable additives such as coolants to find appropriate combinations based on prominent components such as ADN and GAP which help in fine-tuning the optimal formulations in terms of ballistic, mechanical and rheological properties. However, always simultaneous effects on ideal propulsion performance, aggregation/agglomeration phenomena, chemical stability and hazards have to be assessed.

References

- Babuk, V.A., Dolotkazin, I.N., Glebov, A.A., 2005. Burning mechanism of aluminized solid rocket propellants based on energetic binders. *Propellants, Explos., Pyrotech.* 30 (4), 281–290.
- Babuk, V.A., Vasilyev, V.A., Malakhov, M.S., 1999. Condensed combustion products at the burning surface of aluminized solid propellant. *J. Propul. Power* 15 (6), 783–793.
- Beckstead, M.W., Derr, R.L., Price, C.F., 1970. Model of composite solid-propellant combustion based on multiple flames. *AIAA J.* 8 (12), 2200–2207.
- Brewster, M.Q., Mullen, J.C., 2010. Flame structure in aluminized wide-distribution AP composite propellants. *Combust. Flame* 157 (12), 2340–2347.
- Bruno, C., Riva, G., Zanotti, C., Dondè, R., Grimaldi, C., De Luca, L., 1985. Experimental and theoretical burning of solid rocket propellants near the pressure deflagration limit. *Acta Astronaut.* 12 (5), 351–360.
- Cerri, S., Galfetti, L., DeLuca, L.T., D'Andrea, B., Cianfanelli, S., 2007. Experimental investigation of the condensed combustion products of micro aluminized solid rocket propellants. In: *AIAA Paper 2007-5766*.
- Chai, Y., Tao, Z., Jiang, Y., 1995. A study on the catalytic thermal decomposition of sodium azide and correlation with the nitrogen generating propellants' burning rates. *J. Propul. Technol.* 16 (3), 52–56.
- Chakravarthy, S.R., Price, E.W., Sigman, R.K., 1997. Mechanism of burning rate enhancement of composite solid propellants by ferric oxide. *J. Propul. Power* 13 (4), 471–480.
- Chaturvedi, S., Dave, P., 2015. Solid propellant: AP/HTPB composite propellants. *Arab. J. Chem.* <http://dx.doi.org/10.1016/j.arabjc.2014.1012.1033>.
- Cohen, N.S., 1983. A pocket model for aluminum agglomeration in composite propellants. *AIAA J.* 21 (5), 720–725.
- De la Fuente, J.L., 2013. Mesoporous copper oxide as a new combustion catalyst for composite propellants. *J. Propul. Power* 29 (2), 293–298.
- De Luca, L.T., Galfetti, L., Maggi, F., Colombo, G., Paravan, C., Reina, A., Dossi, S., Fassina, M., Sossi, A., 2014. Characterization and combustion of aluminum nanopowders in energetic systems. In: Gromov, A., Teipel, U. (Eds.), *Metal Nanopowders: Production, Characterization, and Energetic Applications*. John Wiley & Sons, pp. 301–410.
- DeLuca, L.T., Galfetti, L., Colombo, G., Maggi, F., Bandera, A., Babuk, V.A., Sinditskii, V.P., 2010. Microstructure effects in aluminized solid rocket propellants. *J. Propul. Power* 26 (4), 724–732.
- DeLuca, L.T., Galfetti, L., Severini, F., Meda, L., Marra, G., Vorozhtsov, A.B., Sedoi, V.S., Babuk, V.A., 2005. Burning of nano-aluminized composite rocket propellants. *Combust. Explo. Shock Waves* 41 (6), 680–692.
- DeLuca, L.T., Price, E.W., Summerfield, M., 1992. *Nonsteady burning and combustion stability of solid propellants*. Progress in Astronautics and Aeronautics, vol. 143. AIAA, Washington.
- Dey, A., Ghorpade, V.G., Kumar, A., Gupta, M., 2014. Biuret: a potential burning rate suppressant in ammonium chlorate (VII) based composite propellants. *Cent. Eur. J. Energ. Mater.* 11 (1), 3–13.
- Dirtu, D., Odochian, L., Pui, A., Humelnicu, I., 2006. Thermal decomposition of ammonia. N_2H_4 – an intermediate reaction product. *Cent. Eur. J. Chem.* 4 (4), 666–673.
- Galfetti, L., DeLuca, L., Severini, F., Colombo, G., Meda, L., Marra, G., 2007. Pre and post-burning analysis of nano-aluminized solid rocket propellants. *Aerosp. Sci. Technol.* 11 (1), 26–32.
- Ghorpade, V.G., Dey, A., Jawale, L.S., Kotbagi, A.M., Kumar, A., Gupta, M., 2010. Study of burn rate suppressants in AP-based composite propellants. *Propellants, Explos., Pyrotech.* 35 (1), 53–56.
- Glotov, O., Zyryanov, V.Y., 1995. Condensed combustion products of aluminized propellants. I. A technique for investigating the evolution of disperse-phase particles. *Combust. Explo. Shock Waves* 31 (1), 72–78.
- Gordon, S., McBride, B.J., 1996. *Computer Program for Calculation of Complex Chemical Equilibrium Compositions and Applications II. User's Manual and Program Description*. NASA Reference Publication.
- Grigor'ev, V., Zarko, V., Kutsenogii, K., 1981. Experimental investigation of the agglomeration of aluminum particles in burning condensed systems. *Combust. Explo. Shock Waves* 17 (3), 245–251.
- Ishitha, K., Ramakrishna, P., 2014. Studies on the role of iron oxide and copper chromite in solid propellant combustion. *Combust. Flame* 161 (10), 2717–2728.
- Jawalkar, S., Kurva, R., Sundaramoorthy, N., Dombe, G., Singh, P., Bhattacharya, B., 2012. Studies on high burning rate composite propellant formulations using TATB as pressure index suppressant. *Cent. Eur. J. Energ. Mater.* 9 (3), 237–249.
- Jayaraman, K., Anand, K., Bhatt, D.S., Chakravarthy, S.R., Sarathi, R., 2009a. Production, characterization, and combustion of nanoaluminum in composite solid propellants. *J. Propul. Power* 25 (2), 471–481.
- Jayaraman, K., Chakravarthy, S., Sarathi, R., 2011. Quench collection of nano-aluminium agglomerates from combustion of sandwiches and propellants. *Proc. Combust. Inst.* 33 (2), 1941–1947.
- Jayaraman, K.V.A.K., Anand, K.V., Chakravarthy, S.R., Sarathi, R., 2009b. Effect of nano-aluminium in plateau-burning and catalyzed composite solid propellant combustion. *Combust. Flame* 156 (8), 1662–1673.
- Klager, K., Zimmerman, G.A., 1992. Steady burning rate and affecting factors: experimental results. In: DeLuca, L.T., Price, E.W., Summerfield, M. (Eds.), *Nonsteady Burning and Combustion Stability of Solid Propellants*, Progress in Astronautics and Aeronautics, vol. 143. AIAA, Washington, pp. 59–109.
- Kohga, M., Okamoto, K., 2011. Thermal decomposition behaviors and burning characteristics of ammonium nitrate/polytetrahydrofuran/glycerin composite propellant. *Combust. Flame* 158 (3), 573–582.

- Krishnan, S., Swami, R., 1998. Effect of catalyst addition on subatmospheric burning surface temperatures of composite propellants. *J. Propul. Power* 14 (3), 295–300.
- Kubota, N., 2007. *Propellants and Explosives: Thermochemical Aspects of Combustion*. John Wiley & Sons.
- Langbein, H., Mayer-Uhma, T., 2009. Phase formation of V_2O_5 - xNb_2O_5 compounds via gels and freeze-dried precursors. *Mater. Res. Bull.* 44 (3), 654–659.
- Liu, T.K., 2005. Experimental and model study of agglomeration of burning aluminized propellants. *J. Propul. Power* 21 (5), 797–806.
- Maggi, F., Bandera, A., DeLuca, L.T., Thoorens, V., Trubert, J.F., Jackson, T.L., 2011. Agglomeration in solid rocket propellants: novel experimental and modeling methods. *Prog. Propul. Phys.* 2, 81–98.
- Meda, L., Marra, G., Galfetti, L., Inchingalo, S., Severini, F., De Luca, L., 2005. Nano-composites for rocket solid propellants. *Compos. Sci. Technol.* 65 (5), 769–773.
- Mezroua, A., Khimeche, K., Lefebvre, M.H., Benziane, M., Trache, D., 2014. The influence of porosity of ammonium perchlorate (AP) on the thermomechanical and thermal properties of the AP/polyvinylchloride (PVC) composite propellants. *J. Therm. Anal. Calorim.* 116 (1), 279–286.
- Parhi, A., Mahesh, V., Shaji, A., Levin, G., Abraham, P.J., Srinivasan, V., 2015. Challenges in the development of a slow burning solid rocket booster. *Aerosp. Sci. Technol.* 43, 437–444.
- Peterson, J.A., Reed, J.R., McDonald, A.J., 1967. Control of pressure deflagration limits of composite solid propellants. *AIAA J.* 5 (4), 764–770.
- Price, E.W., 1984. Combustion of metallized propellants. In: Kuo, K. K., Summerfield, M. (Eds.), *Fundamentals of Solid-Propellant Combustion, Progress in Astronautics and Aeronautics*, vol. 90. AIAA, NY, pp. 479–513.
- Reyes-Labarta, J.A., Marcilla, A., 2008. Differential scanning calorimetry analysis of the thermal treatment of ternary mixtures of ethylene vinyl acetate, polyethylene, and azodicarbonamide. *J. Appl. Polym. Sci.* 110 (5), 3217–3224.
- Robledo-Ortiz, J., Zepeda, C., Gomez, C., Rodrigue, D., González-Núñez, R., 2008. Non-isothermal decomposition kinetics of azodicarbonamide in high density polyethylene using a capillary rheometer. *Polym. Test.* 27 (6), 730–735.
- Salmon, A., 2006. Développement d'une méthode prédictive de calcul des enthalpies de formation en phase solide de molécules organiques – Application aux matériaux énergétiques. Unpublished PhD, Ecole Nationale Supérieure des Mines de Paris.
- Shioya, S., Kohga, M., Naya, T., 2014. Burning characteristics of ammonium perchlorate-based composite propellant supplemented with diatomaceous earth. *Combust. Flame* 161 (2), 620–630.
- Sippel, T.R., Son, S.F., Groven, L.J., 2014. Aluminum agglomeration reduction in a composite propellant using tailored Al/PTFE particles. *Combust. Flame* 161 (1), 311–321.
- Steinz, J., Stang, P., Summerfield, M., 1969. *The Burning Mechanism of Ammonium Perchlorate-based Composite Solid Propellants*. Princeton University, AMS Report No. 830.
- Stoner Jr., C.E., Brill, T.B., 1991. Thermal decomposition of energetic materials 46. The formation of melamine-like cyclic azines as a mechanism for ballistic modification of composite propellants by DCD, DAG, and DAF. *Combust. Flame* 83 (3), 302–308.
- Strunin, V.A., Fedorychev, A., Gunin, S., Klyuchnikov, A., Milekhin, Y.M., Manelis, G.B., 2010. Two-zone model for combustion of a composite solid propellant with a coolant. *Combust. Explo. Shock Waves* 46 (3), 315–324.
- Sutton, G.P., Biblarz, O., 2010. *Rocket Propulsion Elements*. John Wiley & Sons.
- Talawar, M.B., Makashir, P.S., Nair, J.K., Pundalik, S.M., Mukundan, T., Asthana, S.N., Singh, S.N., 2005. Studies on diaminoglyoxime (DAG): thermolysis and evaluation as ballistic modifier in double base propellant. *J. Hazard. Mater.* 125 (1), 17–22.
- Talawar, M.B., Nair, J.K., Pundalik, S.M., Satpute, R.S., Venugopalan, S., 2006. Diaminofurazan (DAF): thermolysis and evaluation as ballistic modifier in double base propellant. *J. Hazard. Mater.* 136 (3), 978–981.
- Taylor, F., Bircumshaw, L., 1956. The thermal decomposition of oxamide. *J. Chem. Soc.*, 3405–3410.
- Teipel, U., 2006. *Energetic Materials: Particle Processing and Characterization*. John Wiley & Sons.
- Williams, G.K., Palopoli, S.F., Brill, T.B., 1994. Thermal decomposition of energetic materials 65. Conversion of insensitive explosives (NTO, ANTA) and related compounds to polymeric melon-like cyclic azine burn-rate suppressants. *Combust. Flame* 98 (3), 197–204.
- Zanotti, C., Giuliani, P., 1994. Pressure deflagration limit of solid rocket propellants: experimental results. *Combust. Flame* 98 (1), 35–45.
- Zhang, X.D., Li, J.M., Yang, R.J., Zhao, X.Q., 2010. Effect of azodicarbonamide on the properties of BAMO-THF/PSAN propellants. *Trans. Beijing Inst. Technol.* 30 (5), 603–607.